Chem Soc Rev

TUTORIAL REVIEW

View Article Online
View Journal | View Issue

Cite this: *Chem. Soc. Rev.*, 2014, **43**, 3244

Advances in radical probe mass spectrometry for protein footprinting in chemical biology applications

Simin D. Maleknia[a] and Kevin M. Downard*[b]

Received 27th November 2013

DOI: 10.1039/c3cs60432b

www.rsc.org/csr

Radical Probe Mass Spectrometry (RP-MS), first introduced in 1999, utilizes hydroxyl radicals generated directly within aqueous solutions using synchrotron radiolysis, electrical discharge, and photochemical laser sources to probe protein structures and their interactions. It achieves this on millisecond and submillisecond timescales that can be used to capture protein dynamics and folding events. Hydroxyl radicals are ideal probes of solvent accessibility as their size approximates a water molecule. Their high reactivity results in oxidation at a multitude of amino acid side chains providing greater structural information than a chemical cross-linker that reacts with only one or few residues. The oxidation of amino acid side chains occurs at rates in accord with the solvent accessibility of the residue so that the extent of oxidation can be quantified to reveal a three-dimensional map or footprint of the protein's surface. Mass spectrometry is central to this analysis of chemical oxidative labelling. This tutorial review, some 15 years on from the first reports, highlights the development and significant growth of the application of RP-MS including its validation and utility with ion-mobility mass spectrometry (IM-MS), the use of RP-MS data to help model protein complexes, studies of the onset of oxidative damage, and more recent advances that enable high throughput applications through simultaneous protein oxidation and on-plate deposition. The accessibility of the RP-MS technology, by means of a modified electrospray ionization source, enables the approach to be implemented in many laboratories to address a wide range of applications in chemical biology.

Key learning points
- The basis of Radical Probe Mass Spectrometry (RP-MS) and how it complements other approaches used to study protein structures and interactions
- Means to generate hydroxyl radicals on millisecond and submillisecond timescales
- The do's and don'ts of exposing proteins to high fluxes of hydroxyl radicals and the direct validation of the approach using ion mobility mass spectrometry
- Application to studies of protein structure, folding events and interactions and advances to model protein complexes and achieve high sample throughput
- Ability to extend reaction timescale to study the onset of oxidative protein damage at a local and global level

1. Introduction

Radical Probe Mass Spectrometry (RP-MS), first introduced 15 years ago in 1999,[1] represents a pioneering approach that utilizes hydroxyl radicals generated directly within aqueous solutions to probe protein structures and their interactions on millisecond and sub-millisecond timescales that can capture protein folding and interaction events.

The concept of DNA footprinting[2] opened the door to its application to study protein structures and interactions that are essential to our understanding of their biological function.[3] Mass spectrometry based methods offer advantages for such studies, over conventional X-ray crystallographic and NMR spectroscopic approaches, as they require far lower levels of sample, in the micromolar and submicromolar range, and can be quickly implemented with higher sample throughput.[4] Importantly, RP-MS offers several advantages over other mass spectrometry approaches widely used to study the structure and interactions

[a] *School of Civil and Environmental Engineering, University of New South Wales, Sydney, Australia*
[b] *Marie Bashir Institute for Infectious Diseases and Biosecurity, University of Sydney, Molecular Bioscience Building G08, Sydney, NSW 2006, Australia. E-mail: k.downard@sydney.edu.au; Tel: +61 (0)2 9351 4140*

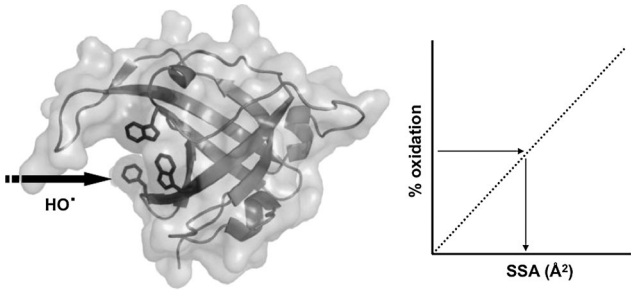

Fig. 1 Basis of Radical Probe Mass Spectrometry (RP-MS) in which oxidation levels at reactive residue side chains correlate with their solvent accessibility.

of proteins in solution[5] ranging from their limited proteolysis,[6,7] hydrogen exchange[8,9] and chemical cross-linking methods.[10,11]

In the late 1990s,[12,13] it was first demonstrated that the surface of proteins could be probed after their limited exposure to hydroxyl radicals. These studies differed from earlier footprinting experiments[14] that studied DNA–protein interactions through the abstraction of hydrogen atoms from the deoxyribose sugars of the DNA backbone, a process restricted at sites when a protein molecule is bound. In the dedicated protein footprinting studies, hydroxyl radicals were found to induce the limited oxidation of certain amino acid side chains, over cleavage of the backbone, throughout a protein's structure. It was found that the level of oxidation was directly correlated with the side chain solvent accessibility (SSA) (Fig. 1).[15,16] The sites and level of protein oxidation could then be identified and quantified by mass spectrometry employing direct mass analysis and tandem approaches utilizing a range of instrument configurations. From this, a three-dimensional map or footprint of the protein's surface could be assembled based upon the oxidation profile. The overall approach (Fig. 2), as described in the original work,[13] was referred to as Radical Probe Mass Spectrometry (or simply RP-MS). This term was also used in the first review of the approach.[16] It is preferred over others, as it is akin to hyphenated descriptions of related methods such as HX-MS,[8,9] and highlights the importance of mass spectrometry to the analysis of the products of oxidation. Others terms make no reference to the essential use of mass spectrometry. These include hydroxyl radical protein footprinting,[15,19] by analogy with earlier footprinting methods,[14] oxidative surface mapping,[20] oxidative labeling, chemical oxidative labeling and photochemical oxidation,[21] all of which describe RP-MS experiments.

Over 15 years on from the initial studies,[12,13] this article highlights the development, and significant growth, of the application of RP-MS since the first review on the subject.[16] It further details the latest approaches to effect hydroxyl radical production, the present understanding of the mechanisms of the underlying radical chemistries, the critical parameters required to affect the RP-MS approach without protein structural perturbation or damage, the development of computational approaches to help manage and interpret the RP-MS data, and the extension of the approach to investigate the onset of protein oxidative damage.

2. Basis of the RP-MS approach and its advantages

RP-MS involves the rapid generation of hydroxyl, in addition to other oxygen-containing radicals, in high flux within several microseconds by photochemical or discharge sources.[15–21] Their subsequent reaction with proteins occurs over several milliseconds that results in their limited oxidation (<10–30% total protein oxidation)

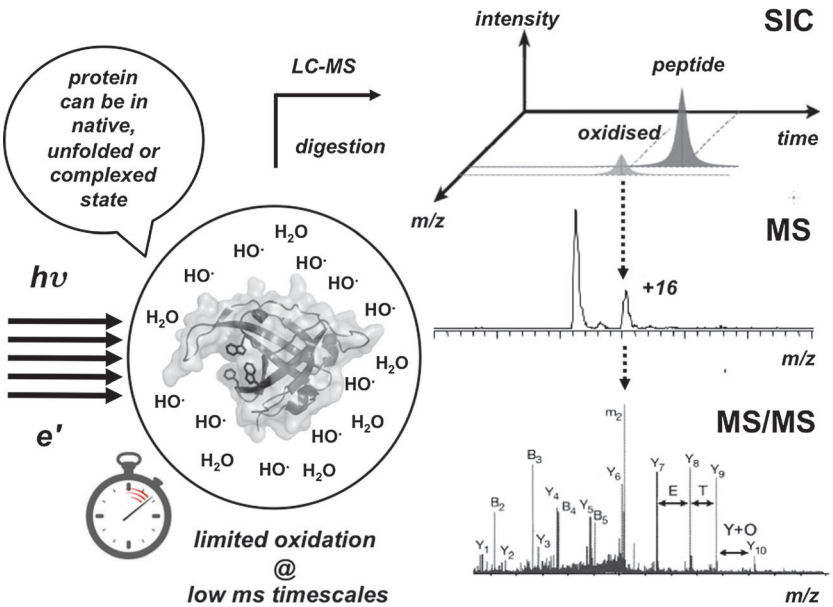

Fig. 2 Overview of the procedures employed in RP-MS experiments to oxidize, digest, quantify oxidation levels and determine the site of oxidation using mass spectrometry.

without any appreciable damage to their structural and conformational integrity. Either the rate or level of irreversible protein oxidation is then measured at the reactive amino acid side chains using mass spectrometry. As the rate, extent and site of oxidation are highly influenced by the solvent accessibility of the reactive residues to the bulk solvent, the RP-MS data can be used to assemble or confirm the three-dimensional structure of a protein's surface including any change to that surface during a folding event or when another biomolecule binds (Fig. 2).

Hydroxyl radicals are ideal probes with which to investigate a protein's structure since they are highly reactive and they approximate the size of a water molecule (approximately 3 Å) from which they are generated in aqueous solution. Their production on short timescales, and their fast reaction rates with amino acid side chains ranging from 10^9 to 10^{10} M^{-1} s^{-1}, enable time-resolved studies of protein folding and interactions to be conducted that are not possible by slower chemical methods.[18,19]

The generation of high fluxes of hydroxyl radicals directly from water was originally accomplished using synchrotron X-ray radiolysis (Fig. 3A).[15] The same researchers developed an alternate means to generate hydroxyl radicals employing an electrical discharge within an electrospray ion source (Fig. 3B) that was published simultaneously.[16] The latter method provides a more convenient, and accessible, means with which to oxidize proteins in RP-MS experiments that has been shown to impart similar levels of oxidation to radiolysis and other photochemical methods.[15,20] Recent studies have confirmed the integrity of protein structures oxidized in this manner through the use of ion mobility mass spectrometry.[22] The electrical discharge approach further enables proteins to be oxidized and simultaneously deposited onto a matrix-assisted laser desorption ionization (MALDI) sample plate to help facilitate rapid sample analysis.[23]

Hydroxyl radicals are highly reactive species and induce the oxidation of amino acid side chains within a few milliseconds. They also target a multitude of residues[12] providing greater structural information than a single cross-linker that targets only one or a

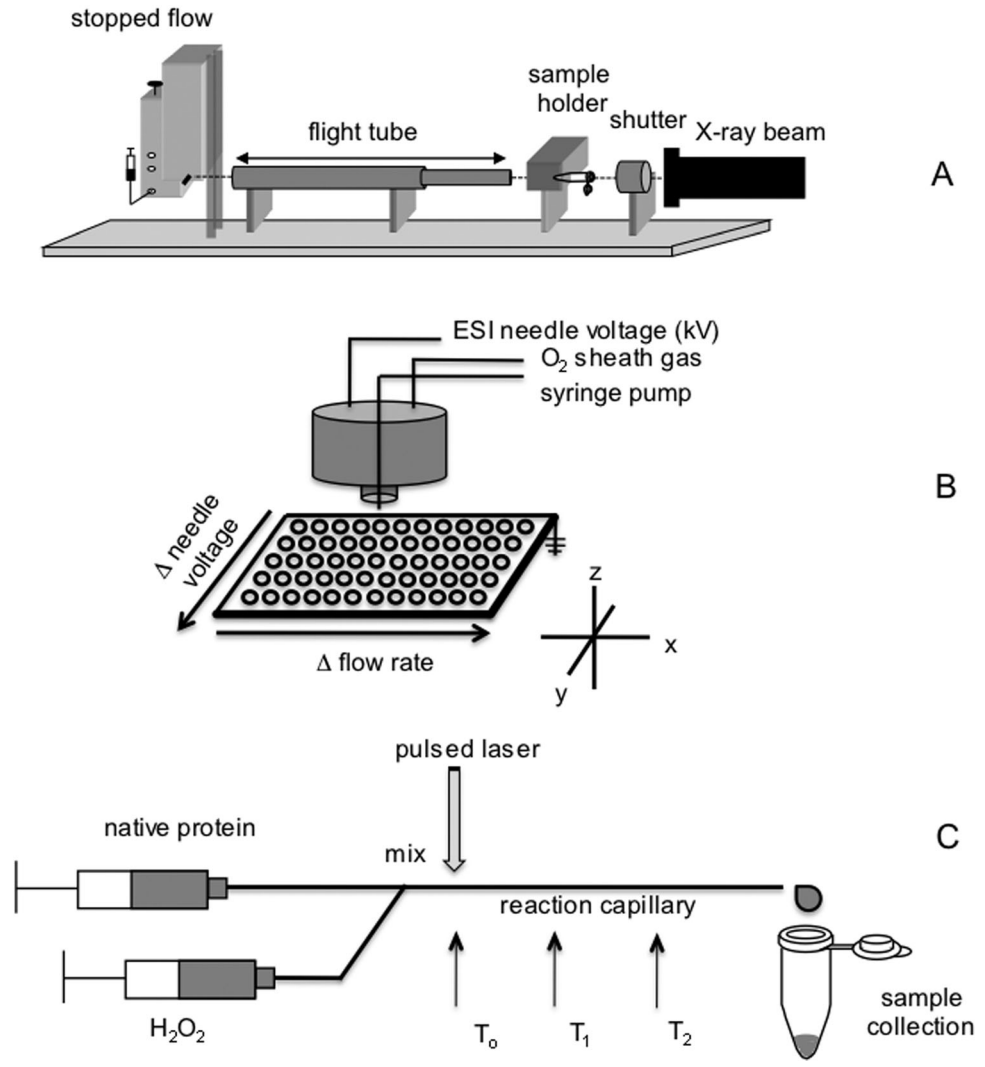

Fig. 3 Approaches employed to generated hydroxyl radicals in solution on millisecond and sub-millisecond timescales for RP-MS experiments.

small group of amino acid residues.[11] The reactions are irreversible, unlike hydrogen exchange,[8,9] and the oxidized products are stable. As a consequence, the use of proteolysis combined with MS and MS/MS analysis, using a tandem mass spectrometer, enables the levels and sites of oxidation at the reactive residues to be determined. Furthermore, the incorporation of mass spectrometric analysis enables samples to be analysed that are not of high purity since the mass resolving power and mass precision achievable with current mass spectrometers enable the protein products to be easily differentiated from any other contaminants in solution.

To preserve the structural integrity of proteins, the hydroxyl radical exposure time should be kept below some 30–50 milliseconds.[16] This important aspect was overlooked by others who sought to employ the approach through the chemical treatment of proteins with high concentrations of hydrogen peroxide.[24] The introduction of such a non-physiological reagent can not only have a deleterious impact on the structural integrity of proteins and their complexes, it also results in high oxidation levels and protein cleavage through the long term presence of hydroxyl radicals. As demonstrated in earlier reports,[16] it is necessary to limit the maximum level of protein oxidation to less than 30% of all protein present. Under these conditions, most protein remains unoxidized, some is mono-oxidized, and even less is oxidized through the incorporation of 2 or more oxygen atoms. Thus a protein population is produced in which total oxidation levels are distributed to differing degrees across the reactive residue side chains such that the oxidation level at any residue is only a few percent or less. It has been determined that reactive amino acid side chains with solvent accessibilities of greater than 30 Å^2 can be oxidized by this approach. This has been shown not to impart any measurable change in a protein's structure.[15–21,23] Increasing the reaction timescale, or the level of oxidation further, results in the onset of protein damage and the formation of both degraded protein and cross-linked protein aggregates.[16]

3. Production of hydroxyl radicals on sub-millisecond to millisecond timescales

3.1 Synchrotron X-ray radiolysis

A synchrotron X-ray radiolysis source can produce a beam of unfocused "white" light that delivers a continuous spectrum of approximately 10^{14}–10^{15} photons per second with energies ranging from 5 to 30 keV (Fig. 3A). Under these beam conditions, the production of hydroxyl radicals occurs within 100 microseconds at a steady-state micromolar concentration. The initial ionization of water requires only about 0.3 mJ of energy and occurs according to eqn (1):

$$2H_2O + e^- \text{ (ionizing radiation)} \rightarrow H_2O^{+\bullet} + H_2O^* + e_{aq}^- \quad (1)$$

Excited water molecules (H_2O^*) dissociate to hydroxyl radicals within 10^{-13} s, and $H_2O^{+\bullet}$ reacts with water to produce more hydroxyl radicals according to eqn (2):

$$H_2O^{+\bullet} + H_2O \rightarrow H_3O^+ + HO^\bullet \quad (2)$$

The electrons produced in eqn (1) become hydrated (*i.e.* e_{aq}^-) within 10^{-12} to 10^{-11} s. The hydroxyl radicals react with protein molecules present, recombine or react with solvent molecules. When such reactions are performed aerobically, superoxide anions and hydroperoxyl radicals can also be generated according to eqn (3) and (4):

$$e_{aq}^- + O_2 \rightarrow O_2^{\bullet -} \quad (3)$$

$$O_2^{\bullet -} + H_2O \rightarrow HO_2^\bullet + HO^- \quad (4)$$

The oxidation of proteins through synchrotron X-ray radiolysis[12,15,16] was achieved through the irradiation of an entire protein solution using a beam width of approximately 5 mm. The exposure times were controlled by means of an electronic shutter for static experiments, or using a stopped flow apparatus for dynamic protein folding/unfolding or protein interaction studies (Fig. 3A).

3.2 Electrical discharge

The electrical discharge source was developed[13] in concert with synchrotron X-ray radiolysis experiments in recognition of the limited availability, restricted access and high costs of synchrotron beamlines. The oxidation of proteins within conventional atmospheric pressure electrospray ionization (ESI) sources require only that the needle voltage be raised from that used during standard operation. Radicals can be conveniently produced in solution at the electrospray needle tip when the voltage difference between the electrospray needle and the sampling orifice of the mass analyzer is increased from typically 4 kV to some 6–8 kV (Fig. 3B). Hydroxyl radicals are produced under these conditions according to eqn (5) in which e^- (H_2O) refers to hydrated electrons:

$$H_2O \rightarrow H_2O^{+\bullet} + e^- (H_2O) \rightarrow H_3O^+ + HO^\bullet + e^- \quad (5)$$

Hydroxyl radical production is supplemented when oxygen replaces nitrogen as the nebulizer gas according to eqn (6):

$$O_2 - e^- (H_2O) \rightarrow O_2^{+\bullet} + (H_2O) \rightarrow H_3O^+ + H_2O \rightarrow HO^\bullet + e^- (2H_2O) \quad (6)$$

The oxidation efficiency of pure oxygen was twice that of air (comprised of approximately 20% oxygen) as demonstrated in electrospray discharge studies of two peptide pentamers.[25] Each peptide contained one of the most highly reactive tryptophan and tyrosine residues. Both were found to oxidize at higher levels when pure oxygen gas replaced air as a nebulizer gas, while all other discharge conditions remained unchanged. This supported the role of oxygen in hydroxyl radical production.

The electrophysical production of hydroxyl radicals can be controlled through altering the discharge conditions. This can be achieved by means of raising or reducing the electrospray needle voltage, controlling the nature of the nebulizer sheath gas, and/or by varying the flow rates of protein solutions through the electrospray needle.[21] Slower solution flow rates lead to proteins having longer residence times at the needle tip and thus result in higher oxidation levels. The reverse is true when the solution flow rate is slowed through the needle. Typical flow

rates of between 1–5 μl min^{-1} are usually employed. While proteins can be analysed directly within the confines of the electrospray mass spectrometer, the condensation of oxidized protein droplets facilitates the subsequent proteolytic digestion and analysis of the peptide products. Where a high resolution FT-ICR mass spectrometer is employed, so-called ''top-down'' tandem mass spectrometry experiments can be performed to identify the sites of oxidation without the need for proteolysis of the oxidized protein.

To improve sample throughput and minimize sample consumption, protein oxidation by electrical discharge has recently been accomplished with the simultaneous on-plate deposition onto a MALDI target.[23] It has been shown that the oxidized proteins can then be proteolytically digested on-plate.[23] In these experiments, the electrospray ionization needle was mounted vertically over a 384-well MALDI plate whose position was adjusted by means of a xyz stage. An external high-voltage supply provided a needle potential sufficient to induce protein oxidation in a controlled manner at 6 kV, where structural integrity is maintained, and up to 9 kV when the onset of oxidative damage was observed.

3.3 Laser photolysis of hydrogen peroxide

The later implementation of the RP-MS approach investigated the use of lasers to generate hydroxyl radicals through the fast photolysis of hydrogen peroxide to minimize exposure to this chemical oxidant.[26–28] Hydroxyl radicals are produced simply according to the photolytic reaction shown in eqn (7):

$$H_2O_2 + h\nu \rightarrow 2HO^{\bullet} \quad (7)$$

When a pulsed UV laser is employed, high concentrations of hydroxyl radicals are produced in nanoseconds (Fig. 3C).[26] Studies have shown that a single laser pulse is all that is required to produce extensive oxidation of a protein surface, and that monooxidized proteins were more susceptible to further oxidation by subsequent irradiation compared to unoxidized molecules.[26] This is associated with conformational change that increases the solvent-accessible surface area of the protein and which are to be avoided in RP-MS studies of protein structures.

While capable of fast hydroxyl radical production, such laser based experiments nonetheless require the addition of high (mM) concentrations of hydrogen peroxide with its concomitant impact on the physiological state of proteins and their complexes. There also remains the need to expel unreacted or reformed hydrogen peroxide after protein oxidation. It is well known that hydrogen peroxide can itself induce protein oxidation without any further stimuli given its instability in solution. If radical scavengers are to be added after reaction, care must also be taken that they do not interfere with the structure of the proteins by creating a non-physiological solution environment.

3.4 Ozonolysis

An alternate method to facilitate the production of solution-based radicals is through the use of ozone. Ozone, or triatomic oxygen, can be generated from diatomic oxygen by electrical discharge or photolysis. When ozone is subsequently bubbled though an aqueous solution, hydroxyl radicals are efficiently generated according to eqn (8):

$$3O_2 + e^- \text{ or } h\nu \rightarrow 2O_3 + (H_2O) \rightarrow 2HO^{\bullet} + O_2 \quad (8)$$

For its implementation as a source of hydroxyl radicals for RP-MS applications, ozone was produced from pure oxygen using a commercial ozonizer.[29] A flow meter was used to adjust the rate of ozone/oxygen gas bubbled into a vial containing an aqueous buffered solution of peptides or proteins in order to control the level of oxidation.

For peptides and proteins, introduction of ozone into a low micromolar concentration peptide solution was sufficient to effect oxidation at residues known to react with hydroxyl radicals.[29] To illustrate, the ESI-MS spectrum of oxidized des-Arg1-bradykinin (of sequence PPGFSPFR) reveals mono to trioxidized products reflecting 40 to 60% total oxidation with increased reaction times (Fig. 4A). The mono-oxidized product at +14 u corresponds to pyroglutamic acid at *m/z* 918.4 while subsequent side chain oxidation of proline or phenylalanine residues gives rise to +16 u products at *m/z* 934.4 and 950.4 respectively (Fig. 4B). In both cases, the oxygen atom incorporated is derived from air as confirmed by radiolysis experiments performed in ^{18}O–water.[12]

4. Reactions of amino acids side chains with radicals

Reactions of oxygen-containing radicals with peptides and proteins have been extensively studied because of their importance in aging and diseases.[30] The reactivity of amino acid side chains in RP-MS experiments was investigated through reactions of a series of peptides with multiple reactive residues when exposed to synchrotron X-rays or an electrical discharge. These studies revealed that hydroxyl radicals react preferentially with the side chains of aromatic, heterocyclic, or sulfur-containing amino acids at rates of between 5×10^9 to 10^{10} M^{-1} s^{-1} (Table 1). In comparison, the reactions of hydroxyl radicals with α-carbon hydrogen atoms leading to backbone bond cleavage are slower (10^9 M^{-1} s^{-1}). The order of reactivity of amino acid side chains was found to be Cys, Met > Trp, Phe, Tyr > Pro > His > Leu ≫ Lys[12,21] where they are equally accessible in the bulk solution. In most cases, the residue side chains are modified through the simple addition of one or two oxygen atoms. This has minimal to no impact on a protein's structure.

Oxidation of methionine can lead to addition of two oxygen atoms on sulfur producing a sulphoxide or sulphone (+16 or +32 u). Interestingly, the single oxidation of cysteine is less favoured with both dioxidized and trioxidized (*i.e.* sulfonic acid) peptides detected as stable products. The oxidation of the side chains of tryptophan, phenylalanine and tyrosine occurs through a common mechanism that commences with hydroxyl radical addition to the aromatic ring leading to

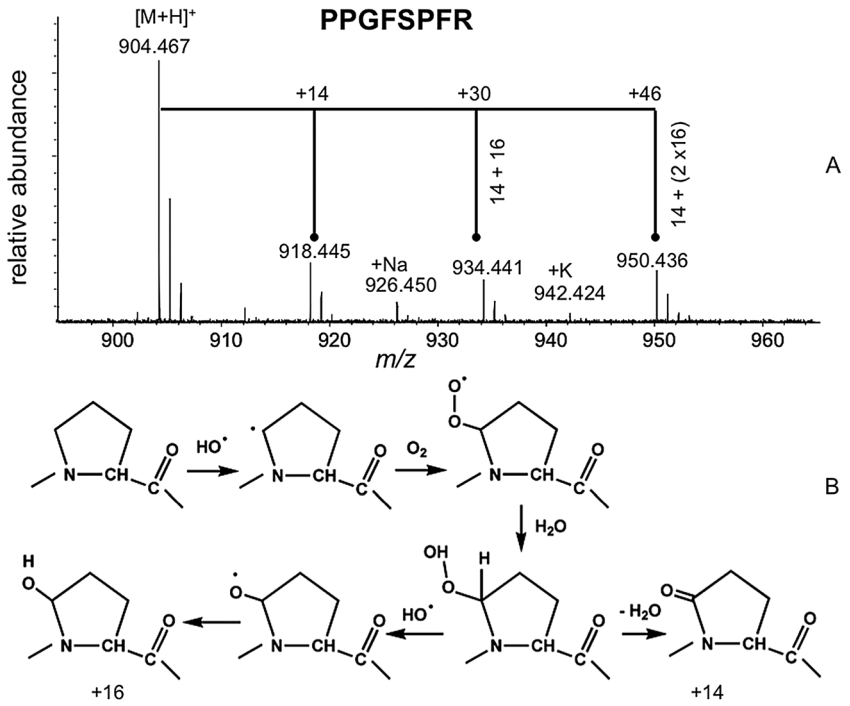

Fig. 4 (A) Electrospray mass spectrum for bradykinin residues 2–9 (PPGFSPFR) after ozonolysis oxidation. (B) Mechanism of oxidation of proline residue(s) contained within peptide.

hydroxylated products. Oxidation of tryptophan side chain can also occur by insertion of hydroxyl radicals into the indole ring leading to the production of a *N*-formylkynurenine product (+32 u).[12] Such multiple oxidation products are common to a number of reactive amino acids. Proline, for example, oxidizes to produce hydroxyproline (+16 u) or pyroglutamic acid (+14 u) products (Fig. 4B).

While oxidation products of leucine and lysine were identified upon the exposure of peptides to hydroxyl radicals,[12,21] they are seldom oxidized in proteins especially with the availability of other more reactive residues (*i.e.* the sulfur-containing and aromatic residues). Overall, there are at least seven amino acids that can serve as solvent accessibility markers (top 7 residues in Table 1). Other residues, such as glycine, alanine, aspartic acid, serine and threonine were reported more recently[31] to react under longer exposure conditions, associated with their slower reaction rates (see Table 1), but are often associated with significant side chain modifications. This can adversely impact on a protein's structure where these side chains play a role in stabilizing the structure through hydrophilic or hydrophobic interactions. This has raised questions about their usefulness as structural probes in RP-MS applications.[19,25]

The reactions of a series of peptides in ^{18}O-labelled water revealed that oxygen from air could also be incorporated in oxidative reactions according to eqn (4) and (5). This is particularly true of methionine, a residue with a known susceptibility to oxidize even when proteins are exposed to air without other stimuli.[25] The rate constants measured for reactions of common amino acids with hydroxyl radicals from low-flux pulsed radiolysis are provided in Table 1. These rates correlate well with the reactivity and selectivity of amino acid oxidation observed in both synchrotron X-ray radiolysis and electrospray discharge experiments.

Table 1 Rate constants for the reaction of the side chains of amino acids with hydroxyl radicals. The top seven, most reactive amino acids are reliable markers of solvent accessibility

Amino acid	Rate constant (M^{-1} s^{-1})
Cysteine	3.4×10^{10}
Methionine	8.3×10^{9}
Histidine	1.3×10^{10}
Tryptophan	1.3×10^{10}
Tyrosine	1.3×10^{10}
Proline	1.2×10^{10}
Phenylalanine	6.5×10^{9}
Leucine	1.7×10^{9}
Alanine	7.7×10^{8}
Valine	7.6×10^{8}
Asparagine	4.9×10^{7}
Lysine	3.5×10^{7}
Arginine	3.5×10^{7}
Glycine	1.7×10^{7}

The reactivity of amino acid residues is highly influenced by their solvent accessibility. This was dramatically demonstrated when the extent of oxidation of amino acids present in the G-helix region of apomyoglobin protein was compared with that for the same 16 residue G-peptide isolated following tryptic digestion of the protein. Oxidation of the G-peptide occurred at phenylalanine and tyrosine residues over histidine, while in the

folded protein the most solvent accessible histidine residues were preferentially oxidized.[25,32]

5. RP-MS studies reveal protein structural preservation

5.1 Level or rate of oxidation correlates with residue side chain solvent accessibility

The validity of the RP-MS method was first demonstrated for lysozyme, a common protein model system. This protein was subjected to oxidation through the independent application of synchrotron radiolysis[15] and electrical discharge.[12] Upon exposure to hydroxyl radicals, oxidized lysozyme was digested and the levels to oxidation across reacted segments of the protein were measured by mass spectrometry. The sites of oxidation were determined by tandem MS/MS experiments. Oxidation levels at reactive residues were compared to the theoretical accessible solvent areas (ASA) of the residue side chains as calculated by the VADAR (Volume, Area, Dihedral Angle Reporter) algorithm[33] using the PDB structure (1E8L) which represents and average of 50 structures of lysozyme in solution as determined by high resolution NMR spectroscopy.

Results of the synchrotron based studies,[15] gave rise to dose response profiles that reflect oxidation levels as a function of the time of exposure. From these profiles, first-order oxidation rates across various tryptic and endoproteinase Glu-C peptide segments were found to differ and reflected the accessibility of reactive residues within those segments (Fig. 5A).

In one such peptide, tandem mass spectrometry confirmed that oxidation occurred exclusively at the most accessible of two neighbouring tryptophan residues at positions 62 and 63. The accessible surface area (ASA) for the side chain of the tryptophan residue at position 62 (124.4 Å^2) is five times that of a like tryptophan residue at position 63.[15] The ESI-MS/MS spectrum for the doubly oxidized tryptic peptide comprising residues 62 to 68 showed the b_5 fragment ion to increase in mass by +32 units, while no change was observed for the y_2 to y_6 fragment ions that did not contain residue Trp-62 (Fig. 5B). This supports the exclusive oxidation of Trp-62.[12] The same result was evident upon application of the electrical discharge approach. Results from both studies similarly revealed, in the case of tryptic segment 34–45, that oxidation occurred at a phenylalanine residue at position 34 (ASA = 40.3 Å^2) and not at phenylalanine at position 38 whose side chain is far less accessible (ASA = 6.2 Å^2).[13,15]

Results of recent on-plate electrospray discharge oxidation with simultaneous deposition for MALDI-MS based analysis, also revealed a close correlation between oxidation levels and the accessibility of the side chain of reactive amino acid residues to the bulk solvent. Using a needle voltage of 6 kV, the level of oxidation within tryptic peptides 22–33, 34–45, 46–61, 62–68/73, 115/117–125 was found to have a linear correlation to the accessibility of reactive residue side chains (Fig. 6). For example, the tryptic peptide 22–33 did not oxidize, consistent with a near zero ASA value for residue Trp-28, the segments 62–68 and 62–73 (with one missed cleave site) containing residue Trp-62 (124.4 Å^2) was fully oxidized. The tryptic peptides 117–125 and 115–125

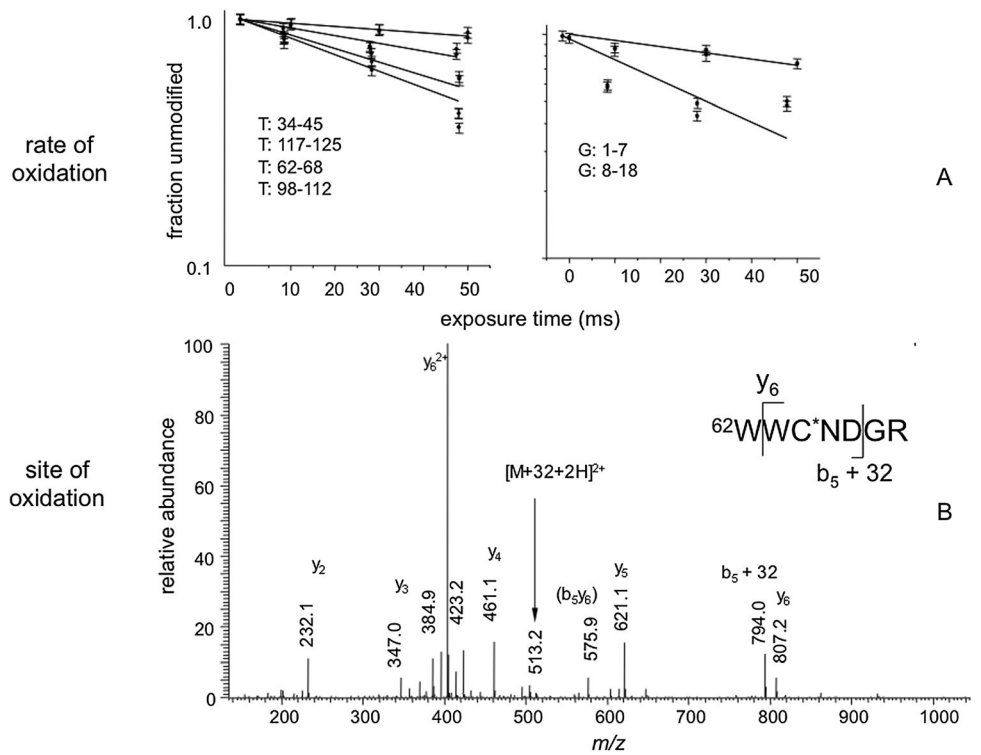

Fig. 5 (A) Rate of oxidation measured within tryptic (T) and endoproteinase Glu-C (G) segments of lysozyme as a function of X-ray exposure time. (B) Site of oxidation determined from MS/MS spectrum illustrated for the dioxidized tryptic peptide 62–68. C* denotes the cysteine residue was alkylated with iodoacetamide.

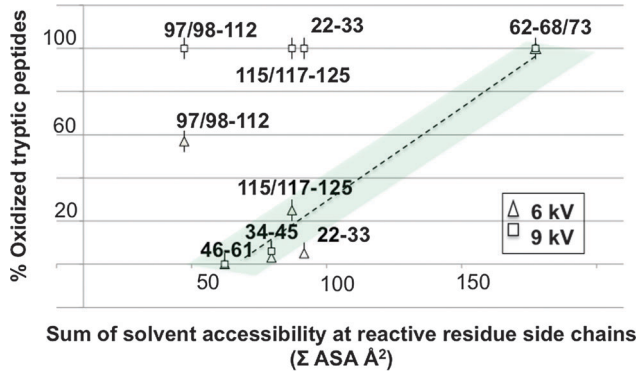

Fig. 6 Level of oxidation within tryptic peptides of lysozyme compared to the solvent accessibility of their reactive residue side chains following oxidation of the protein by electrical discharge with subsequent on-plate deposition at a needle voltage at 6 kV (Δ) and 9 kV (□). The central (green) band shows the region in which oxidation correlates with solvent accessibility and where the structure of the protein is maintained. The data reflects an average of three replicate experiments.

(with one missed cleaved site) was oxidized at near 25% consistent with the accessibility of Trp-123 being between that of the other two (ASA = 77.2 Å^2). The only peptide to deviate was that which contained methionine (97/98–112), a residue that is noted above to rapidly oxidize in air.[12]

At 9 kV, considerable denaturation of the protein is evident as all but two peptides exhibit much higher levels of oxidation. This oxidative damage is shown to occur exclusively towards both termini, as peptide segments in the centre of the protein consisting of residues 34–45, 46–61, and 62–73 are unaffected (Fig. 6). Thus this RP-MS approach can detect local over global oxidative damage and can identify those surface regions of a protein that are most susceptible. By extension, it can also be applied to investigate how a protein in complex is protected from oxidative damage. The ability of antioxidants to mitigate this damage can also be studied by RP-MS as has been reported in the case of *N*-acetylcarnosine.[34]

5.2 Direct evidence of the conformational integrity of oxidized proteins by Ion Mobility Mass Spectrometry (IM-MS)

To directly establish that the proteins oxidized in a limited manner by hydroxyl radicals in RP-MS experiments maintain their conformational integrity, ion mobility mass spectrometry (IM-MS) has recently being employed.[22] IM-MS enables the rotational average collision cross sections (CCS) of proteins in their unoxidized and oxidized states to be studied based on the time that their ions take to drift, or be accelerated, through the high-pressure drift region of a mass spectrometer.[35] Protein ions with a smaller average collision cross section experience less drag and undergo fewer collisions with gas molecules in this region of the instrument. They are therefore detected in advance of protein ions with larger average collision cross sections. Proteins with the same or similar cross sections, will have the same or similar drift or arrival times to the detector.

The effect of the limited hydroxyl radical-induced oxidation on the structure of two model proteins, lysozyme and ubiquitin, was investigated by using a travelling-wave ion mobility instrument.[22] The proteins were oxidized by the electrospray discharge method. The radical-induced oxidation of lysozyme resulted in the incorporation of up to 8 oxygen atoms (Fig. 7A). Ion mobility arrival times were obtained for each of the multiply charged ions of the unoxidized and oxidized forms. Arrival times of some 7.9–9.3 ms were common to all unoxidized and oxidized forms. The measured cross sections, correcting for the effect of charge, was 1722 and 1374 Å^2 for the most predominant 8+ and 7+ ions respectively (Fig. 7B) regardless of their oxidation state. This confirmed directly that their structures were not dissimilar. Note that the 7+ ions, for both the unoxidized and oxidized protein, adopt a more compact protein conformation due to the reduced interaction of like charges within the protein ion. Both measured average cross sections are larger than those theoretically calculated using the projection approximation (PA) method which has been found to underestimate molecular cross sections.[36] This simple approximation to the collision integral describing an ion colliding with hard sphere buffer gas atoms measures the ''shadow'' as the conformer is rotated through all possible orientations.

As lysozyme contains four disulfide bonds, the study of a protein whose structure is not constrained by such bonds was also investigated. Once again, no significant change to the cross sections for the predominant 5+ and 6+ ions of the unoxidized and mono-oxidized forms of the protein was observed. The oxidized proteins therefore shared a common collision cross section to their unoxidized counterparts. Results for both proteins supported that there is no significant change to their global structure during their limited radical-induced oxidation.

6. Application of RP-MS to study protein folding/unfolding

The stability of a protein's tertiary structure is governed by intramolecular forces, which include hydrogen bonds, hydrophobic and electrostatic interactions, between atoms of the amino acid side chains and backbone. A protein is further stabilized, in some cases, by the presence of covalent disulfide bonds between cysteine residues.

The application of RP-MS to study protein folding/unfolding was first demonstrated in 2001 for the protein apomyoglobin.[37] This study simultaneously investigated the thermodynamic unfolding of several regions of the protein in response to different levels of denaturant added to the solution. The level of oxidation in peptides contained within helices A to C, and G was plotted against the urea concentration for various helices (Fig. 8). The unfolding of helix A, comprising residues 1–16, was followed based upon a measure of the oxidation of tryptophan residues at positions 7 and 14 within this segment. Residues 17 to 42 span the B and C helices and contain the reactive residues His24, Phe33, Phe36, and Pro37. The unfolding of this region of the protein was found to be similar to the A-helix, reflecting the cooperative unfolding of the protein. Results for the G-helix, in contrast, demonstrated a distinct local unfolding behavior.

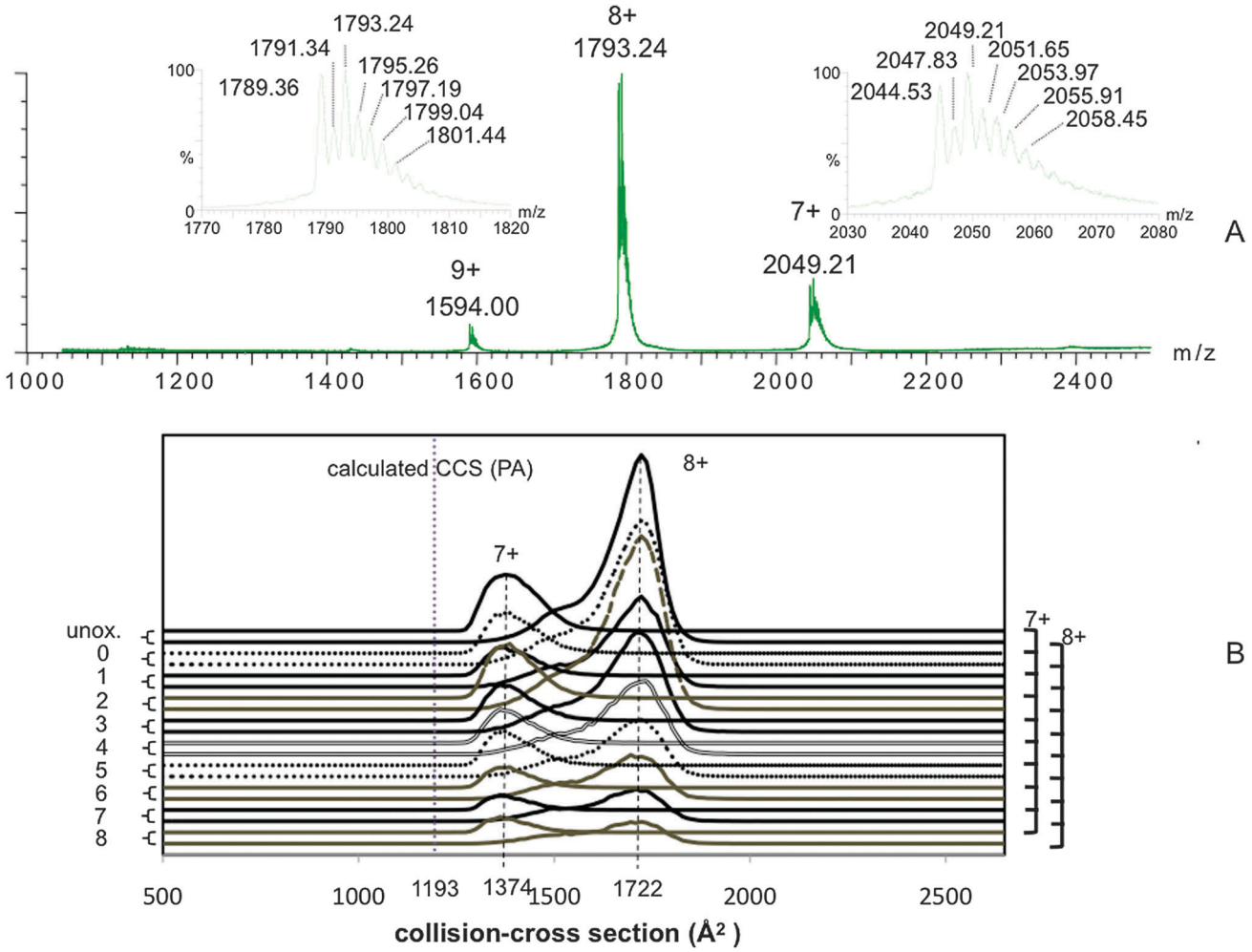

Fig. 7 (A) Electrospray mass spectrum of hen egg lysozyme after oxidation by electrical discharge, and (B) the rotational average collision cross-sections measured for unoxidized and oxidized forms of the protein by ion mobility mass spectrometry.

The midpoint urea concentration, free energy of unfolding, and m values were calculated from all plots. Comparable results have been observed by NMR and Raman spectroscopy; the latter study investigating the protein's acid-induced denaturation.[38]

More recently, the acid-induced unfolding of myoglobin has been followed employing laser-induced oxidation.[39] The stepwise unfolding of helices was followed over a range of exposure times from 50 to 500 ms within the first 50 ms, unfolding was again observed in helix A, a section of the helix B, and the helices C/D. However, the protein's structure was retained in helices E–G. Indeed, the helical BEF core remained partially folded, even after 500 ms, at which point helix G was fully unfolded and exposed to solution.[39]

7. Studies of protein interactions by RP-MS

When proteins bind to other biomolecules, regions of the protein at the interaction interface become protected from the solvent. Thus reactive amino acids at the interface will either not react or react to a lesser degree when exposed to hydroxyl radicals in the solution. The oxidation of proteins alone, and in complex, can be performed by RP-MS under a variety of solution conditions (*i.e.* using various buffers, metal ions, pH's and temperatures) that may promote or disturb the interaction. A map of solvent exposed and shielded amino acid residues enables the binding sites to be determined based on the extent of oxidation under binding and non-binding solution conditions. It is important to monitor oxidation levels at non-binding sites in these studies in order to ensure that the oxidation conditions for the protein alone and in complex were maintained, as the number of potential oxidation sites increases with the increasing number of binding partners present in solution. It has been demonstrated that the RP-MS approach can be applied to the study of protein complexes with dissociation constants (K_d) in the nanomolar range. The first application of RP-MS employing an electrical discharge source to study a non-covalent protein complex was reported in 2003.[40]

7.1 Protein–peptide complexes and a protein docking algorithm developed for use with RP-MS data

The pH-dependent competitive binding of ribonuclease S-protein to S-peptide by RP-MS was examined by adding S-protein to a

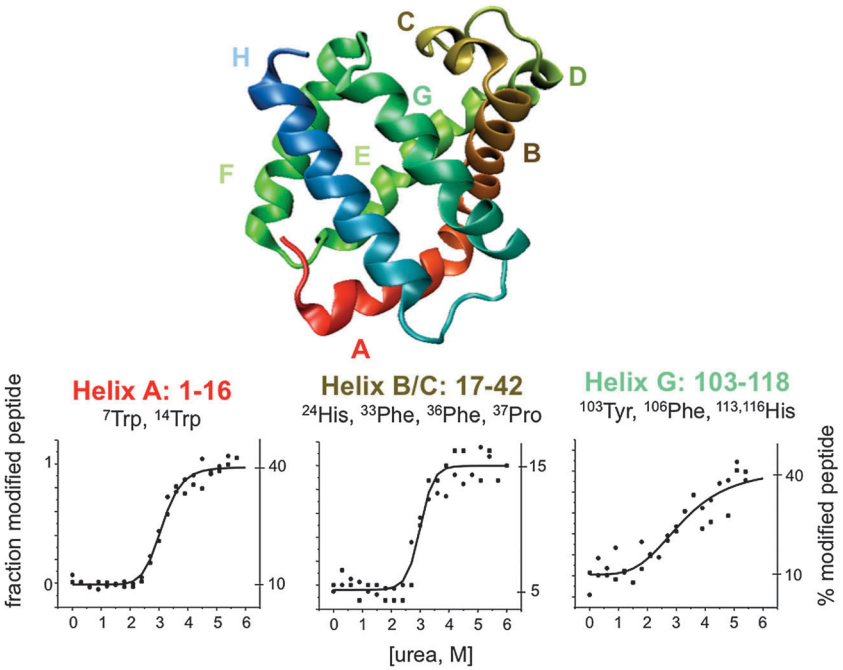

Fig. 8 Helices of the protein apomyoglobin and the urea-induced unfolding of three helical domains followed by RP-MS.

solution containing the ribonuclease S-peptide together with four other non-binding peptides at pH 2 and pH 5.5.[40] Both solutions were subjected to radical induced oxidation by electrical discharge. The percentage of oxidation calculated, from the subsequent ESI mass spectra, revealed comparable oxidation of the non-binding peptides at either pH, while the oxidation of the S-peptide was five-fold greater at pH 2 than at pH 5.5 (Fig. 9A). Tandem mass spectrometry revealed the oxidation of residues Phe8, His12 and Met13 within the S-peptide, all being highly reactive to hydroxyl radicals when S-peptide is released from the complex at a solution pH of 2.

The peptide was found to shield residues 96 to 100 of the S-protein when in complex at pH 5.5. The oxidation level within this segment of the S-protein decreased two-fold upon binding of the S-peptide. The data was input into the PROXIMO (for PRotein OXidation Interface MOdeller) algorithm[41] to generate several modeled structures for the complex (Fig. 9B) based upon a correlation between the solvent accessible surface areas of residues side chains and the oxidation levels measured by RP-MS. Differences in the levels of oxidation at reactive residues in the proteins alone and in complex, together with a geometric fitting routine, are used to assemble and score the models of the protein complex. Impressively, the algorithm revealed the five highest ranked structures were within 1.3 Å^2 (based on with RMSD values) of the reported crystal structure.[41]

Another pH dependent study[42] revealed the specific, calcium-dependent interaction of protein calmodulin with the peptide melittin. When in competition with two other non-binding peptides, only the oxidation of melittin was found to differ at pH 4 and 7. The level of oxidation of melittin increased by

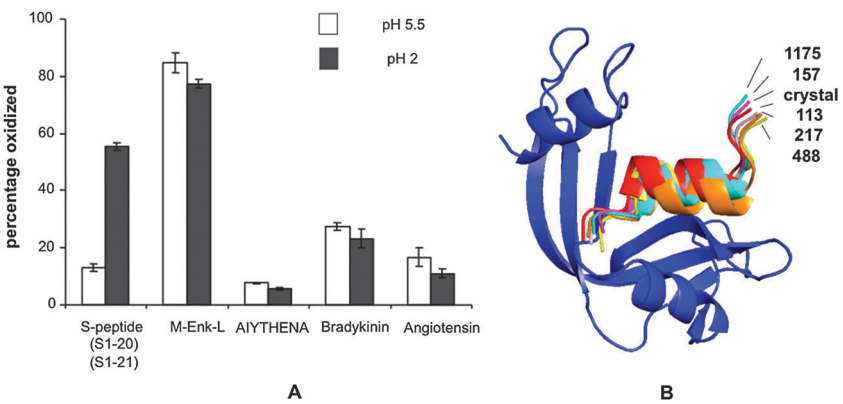

Fig. 9 (A) Oxidation levels measured within five peptides in a mixture with ribonuclease S-protein at pH 5.5 and 2 showing the selective protection conferred to the S-peptide. (B) Top five-ranked structures for the ribonuclease S-protein–S-peptide complex produced by the PROXIMO algorithm using the RP-MS data together with the X-ray crystal structure.

approximately 30% at pH 4 consistent with dissociation of the calmodulin–melittin complex and exposure of reactive residues, particularly Trp-19 residue, within the peptide to more oxidation.

The interaction sites identified within calmodulin, when bound to melittin, were consistent with other theoretical and experimental models of the structure of the complex. The N-terminal domain, up to residue 36, and tyrosine at position 99 in calmodulin were protected from oxidation when melittin was bound at pH 7. Oxidation levels were found to decrease by some 60% within segments 14–21 and 95–106 at this pH. In addition, the formation of the complex induced structural changes in calmodulin resulting in the increased oxidation of phenylalanine residue at position 92 through greater exposure of its flexible loop domain. The RP-MS oxidation data was used in conjunction with PROXIMO algorithm[41] to show that melittin was partially buried within the hydrophobic channel of calmodulin when in complex.[41]

7.2 Protein–protein complexes

The first protein–protein complex studied by RP-MS technique was the Ca^{2+}-dependent binding of actin to a subunit of gelsolin.[16,43] Actin is a 42 kDa globular protein, referred to as G-actin, which transforms into cytoskeletal filaments, denoted F-actin, inside eukaryotic cells. The transformation of G-actin into F-actin mediates cell shape and essential cellular processes such as vesicular transport and cytokinesis.

Gelsolin is an 82 kDa protein with six homologous subdomains (S1 to S6) that regulates actin filamentation by binding with high specificity to actin and severing cross-linked filaments, or acting as a nucleating site for actin polymerization.

As an illustration, oxidation rates for two peptides of gelsolin-S1, one in the binding pocket with actin and the other in a non-binding domain as a control, were examined by RP-MS utilizing synchrotron radiation for hydroxyl radical production (Fig. 3). The oxidation rate for the former peptide of gelsolin-S1 containing residues 96–108, and a reactive phenylalanine residues at position 104, was reduced by a factor of 35 when it was oxidized in the presence of actin *versus* when it was oxidized alone. In contrast, oxidation rates for a peptide segment containing residues 66–83 with a non-binding domain were unaffected.

The calcium-dependent activation of gelsolin was later followed across all its six subdomains.[44] Synchrotron radiolysis of gelsolin in the absence or presence of calcium, identified 7 of a total of 22 peptide segments whose oxidation was calcium dependent. Equilibrium titration isotherms produced by monitoring oxidation levels as a function of calcium concentration, were measured in peptides within subdomains S1, S2, S4 and S6. The stability (K_d) of these domains ranged from 60.4 ± 17.8 μM (for peptide 162–166 of subdomain S2) to 97.3 ± 5.2 μM (for peptide 49–72 of subdomain S1) as measured based upon the midpoint of each transition. The study[44] provided evidence for three-state calcium-dependent activation of the gelsolin subdomains with an intermediate state detected at a calcium concentration of 10 mM.

The complexes of a family of proteins known as crystallins have also been studied by RP-MS. The proteins are so named as they make up the majority of the protein portion of the lens in the eye of animals and are important to maintaining its optical properties. α, β and δ-crystallins are common to most animals, while taxon-specific ones are present in the eye of some species and confer specific functions to the eye, such as to aid an animal's vision at night or underwater. These abundant soluble proteins within the vertebrate eye lens associate into dimers, tetramers and higher-order aggregates that are important for maintaining lens transparency and protecting individual subunits from oxidative damage.

A recent study reported the successful application of RP-MS, in conjunction with ion mobility mass spectrometry, to reveal new findings into the structure of a βB2B3-crystallin complex.[46] The direct detection of the βB2B3 heterodimer by ESI-MS under native conditions was first reported in 2009.[45] The mass spectral data revealed the presence of the homodimer βB2B2 and heterodimer βB2B3, but no evidence for the βB3 monomer or βB3B3 dimer.[46] Thus when a mixture of the βB2 and βB3-crystallin subunits was oxidized, the oxidation of βB3 reflects the protection it is afforded by βB2-crystallin within the heterodimeric complex.[46]

Homology based models, using a structure for the βB2 monomer extracted from that for its tetramer, were built for the βB2B3 heterodimer to find that in which the total ASA of reactive amino acid residue side chains correlated with the total oxidation levels measured within peptide segments of the βB3 subunit.[46] Total oxidation levels ranged from 0 to 100% across six peptide segments of βB3 within the βB2B3 heterodimer. While none of the four homology modeled structures satisfied the oxidation levels measured across the entire protein, particularly in the C-terminal domain, the modeled βB2B3 AD heterodimer provided the best first (Fig. 10). In this model, a βB2 monomer (A) was coupled to N-terminal and C-terminal domains of separate nonadjacent βB2 subunits of the βB2B2 homodimer connected by an elongated linker region. In the AD model, the βB2 and βB3 subunits are positioned further apart along the interacting interface that comprises the RQ plane. The calculated collision cross section based on the 10 lowest energy forms of this model (3139.70 ± 25.40 Å^2) was also in closest agreement with the value measured by ion mobility mass spectrometry (3165 Å^2) (Fig. 10).

8. Measurement of the onset of protein oxidative damage by RP-MS

As demonstrated earlier,[16] the oxidation of proteins on short (10–50) millisecond timescales prevents any significant protein structural perturbation or damage. The use of reactive hydroxyl radicals as a structural probe in RP-MS experiments, however, also allows for the study of the onset of protein damage. Hydroxyl radicals, and other reactive oxygen species (ROS), are a normal outcome of aerobic cellular metabolism and the exposure of living systems to radicals induced by the environment can also contribute to the oxidative damage of biological molecules. Protein oxidative damage and degradation

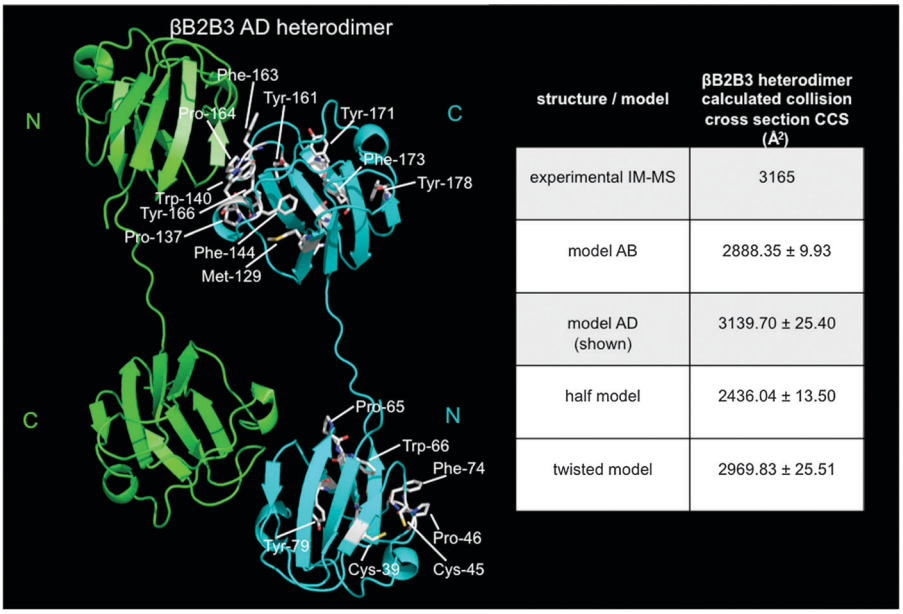

structure / model	βB2B3 heterodimer calculated collision cross section CCS (Å²)
experimental IM-MS	3165
model AB	2888.35 ± 9.93
model AD (shown)	3139.70 ± 25.40
half model	2436.04 ± 13.50
twisted model	2969.83 ± 25.51

Fig. 10 Lowest-energy structure for the AD model of the βB2B3 heterodimer complex AD produced through homology modeling based on RP-MS and ion mobility mass spectrometric data.

have been associated with a range of human diseases and aging processes.[47]

The damage imparted on a protein following its extended (up to 100 milliseconds) reaction of radicals using RP-MS was first demonstrated for apomyoglobin.[16,21] Based on the intensity of bands recorded by gel electrophoresis (Fig. 11A),[16] a plot of total oxidation products with increasing reaction times reveals an initial rise in the level of oxidation ahead of a fall associated with a corresponding increase in levels of both the degraded and cross-linked products (Fig. 11B).[21] The maximum oxidation levels occur at a reaction time of approximately 50 ms. Hence this time represents the limit at which proteins should be exposed to hydroxyl radicals in order to preserve protein structures. By extending the reaction timescale beyond this time, the onset of oxidative damage to proteins can be studied by RP-MS together with its implications for structural and functional damage.

For radiolysis or photolysis based experiments, the reaction timescale is conveniently controlled by use of a shutter. For the electrical discharge approach, the reaction time can be adjusted by controlling the flow rate of protein solutions through the ESI discharge needle or through an increase to the needle voltage. In an example of this latter approach, the oxidation and simultaneous on-plate deposition of lysozyme was studied using two different needle voltages (6 and 9 kV). At the higher voltage, oxidation measured in the peptide segments comprised of residues 22–33, 62–68/73, 97/98–112, and 115/117–125 deviated from the linear correlation with residue side chain accessibility that was observed when 6 kV was applied to the needle (Fig. 6). This demonstrated the onset of oxidative damage within sections of protein most susceptible to such damage, through perturbation of the protein's structure from its native form.

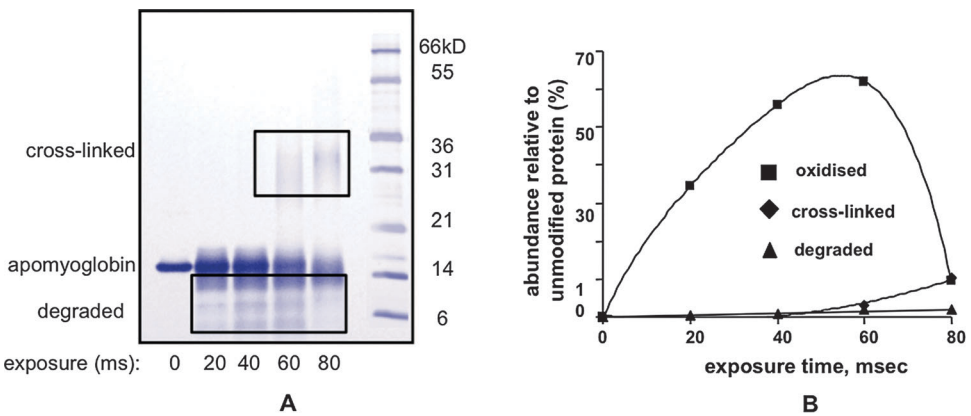

Fig. 11 (A) Evidence for the production of cross-linked and degradation products after more than 0 to 80 millisecond exposure of protein apomyoglobin to hydroxyl radicals, and (B) plot demonstrating the onset of oxidative damage.

8.1 Early onset oxidative damage to lens tissue proteins by RP-MS

Within the lens of the human eye, α-crystallin makes up some 35% of the total protein content. Exposure of the eye to UV light induces significant oxidation, oxidative denaturing, cross-linking and degradation of this and other lens crystallins. These insoluble products adversely impact vision and their accumulation in the eye leads to cataract formation, a leading cause of blindness throughout the world.

Since hydroxyl radicals and other ROS have been implicated directly in nuclear cataract formation, α-crystallin is a good model protein to study its early onset oxidative damage by RP-MS.[48] α-Crystallin was subjected to oxidation under low to high oxidizing conditions using an electrospray discharge source. The extent of oxidation was monitored across all reactive residues in both subunits αA-crystallin and αB-crystallin as a function of oxidizing conditions (Fig. 12).

The level of oxidation was controlled by adjustment of the flow rate of protein solutions passed through the discharge needle. The onset of damage within peptide segments, produced from the subsequent proteolytic digestion of the oxidized protein, occurs at the point at which there is a decrease in oxidation levels at longer reaction times (see arrows in Fig. 12). This occurs due to the production of cross-linked and degradation products. When oxidation levels are plotted as a function of reaction time or flow rate, bell-shaped curves for each peptide were produced,[48] as was previously observed when oxidative damage was detected within the intact protein apomyoglobin (Fig. 11).[32]

The initial sites of oxidation occurred in five regions of subunits αA-crystallin and αB-crystallin (Fig. 12). These comprised the N-terminal residues of 1 to 11 for both subunits A and B, the central domains of subunit B (residues 57–69) and subunit A (residues 104–112), and the C-terminal subunit A (residues 120–145). The C-terminal segment comprising residues 120–145 was most prone to early onset damage, and this was partially attributed to the reduced reactivity of the residues tyrosine, histidine, and isoleucine leading to preferential backbone cleavage. The N-terminal domains within both subunits were found to be more susceptible to oxidative damage with earlier onset times than was evident for the central domains. Note that the level of oxidation that can be accommodated with each protein segment may differ before any oxidative damage is occurs.

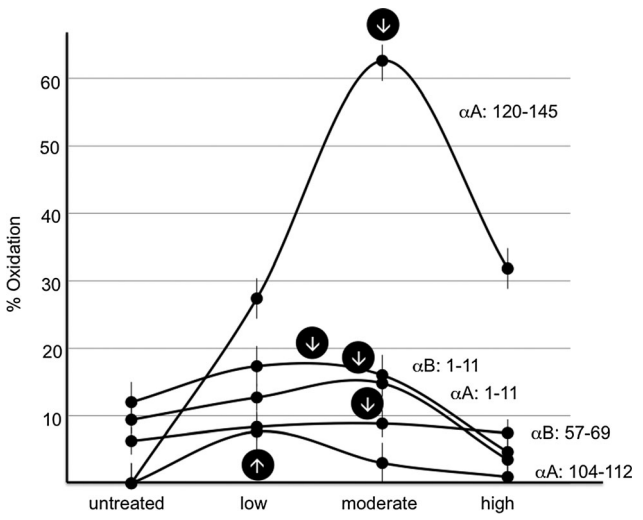

Fig. 12 Oxidation levels within five tryptic peptide segments of the A and B subunits of α-crystallin as a function of oxidizing condition showing differences in the oxidative damage onsets and degree of oxidation ahead of damage.

A similar study was undertaken to examine the protection conferred to a taxon-specific upsilon(υ)-crystallin upon its binding to α-crystallin.[49] The interaction of α and υ-crystallin was first confirmed by native shift gel assay and the radical-induced oxidation of α-crystallin alone and in the presence of υ-crystallin at a ratio of 2 : 1 was performed using the electrical discharge approach under low to high oxidizing conditions. While two of the six oxidized segments of υ-crystallin were unaffected, and thus not protected by the presence of α-crystallin, the remaining four comprising residues 22–41, 132–148, 212–227, and 245–264 were protected by α-crystallin thus delaying the onset of oxidative damage.

9. Application of RP-MS to study impact of oxidation on protein aggregation

Protein aggregation can result in the formation of insoluble deposits and fibrils that have been linked to specific diseases including Alzheimers, Parkinsons, atherosclerosis and rheumatoid arthritis. This aggregation can be affected by protein oxidation. The use of RP-MS to investigate the effects of amino acid side chain oxidation on the kinetics of fibril formation in the case of the protein transthyretin has been reported.[50]

Transthyretin (TTR) is a homotetrameric protein (55 kDa) synthesized primarily in the liver and present in the blood and cerebrospinal fluid. The process of amyloid fibril formation of TTR initiates with tetramer dissociation and partial subunit misfolding, which results in the accumulation of unstructured monomers and their assembly into oligomers.

The effect of amino acid side chain oxidation on the rate of fibril formation was studied for the wild-type (WT) and a TTR mutant (V30M) previously shown to have enhanced rates of fibril formation.[50] To effect complete oxidation, without unoxidized protein remaining, the proteins were oxidized in 3% hydrogen peroxide on a timescale ranging from 10 minutes to one hour. This resulted in the incorporation of up to 5 oxygen atoms, with the mono and dioxidation of methionine residues at position 13 and 30 being the dominant products.

The effect of this oxidation was investigated by comparing the *in vitro* fibril formation of WT-TTR and V30M-TTR in their unoxidized and oxidized forms. The rates of fibril formation were monitored by turbidity assays and absorbance measurements at 330 nm. The results showed that the oxidized proteins could still form fibrils, albeit at a much lower rate than for their unoxidized counterparts (Fig. 13). Oxidation had a more dramatic effect on kinetics of fibril formation for the V30M-TTR

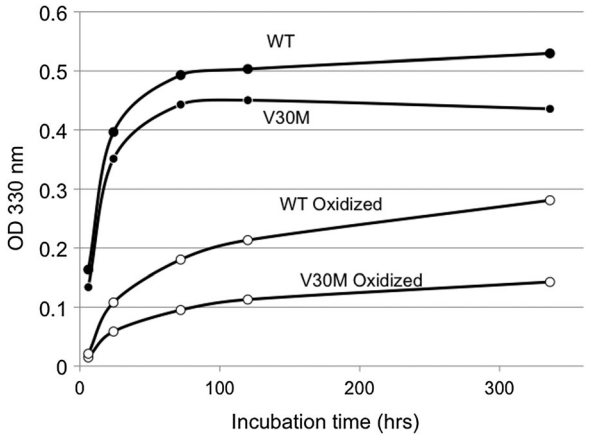

Fig. 13 Kinetics of fibril formation monitored at 330 nm for the wild type (WT) and V30M mutant of transthyretin (TTR) after its reaction with hydrogen peroxide.

mutant *versus* the wild type protein. This is consistent with the fact that the former contains one additional oxidizable methionine residue. The inhibition of fibril growth due to protein oxidation suggests that domains neighboring the methionine residues are critical in stabilizing the tetrameric and folded monomer structures.

10. Conclusions

Radical probe mass spectrometry (RP-MS) has proven itself to be a powerful method for investigating protein structures, studying the dynamics of single proteins and larger assemblies, and characterizing and modeling protein interactions. Additional applications include those to unravel the onset of protein oxidative damage, at the local and global level, and provide insights into the effects of oxidation on the formation of protein aggregates that may impede protein function and lead to the pathogenesis of disease.

The hydroxyl radical provides a convenient probe of solvent accessibility across a multitude of amino acid side chains without the extensive modification inflicted with larger chemical labels in chemical cross-linking studies. Ion mobility mass spectrometry has directly shown that the incorporation of a limited number of oxygen atoms does not result in any detectable change to a protein's structure. This, together with reaction times that can be controlled from low to high milliseconds, enables the approach to be "fine tuned" for a specific protein system, notwithstanding the noted cautions about the effects of exposing proteins to radicals over some 50 ms in order to prevent or minimize protein damage.

Importantly, the RP-MS approach also does not require proteins to be highly purified since the mass resolving power of current mass analyzers, and the potential to incorporate chromatographic separation by means of LC-MS methods, enables the oxidative products to be resolved and identified regardless of the presence of contaminating species. Furthermore, the use of a modified electrical discharge source enables oxidized proteins to be analyzed by ESI-MS, and this same source can be used to effect the simultaneous oxidation and on-target deposition of proteins to facilitate high sample throughput employing MALDI-MS. The availability of algorithms to help model proteins and their complexes using RP-MS data should help to sustain and even accelerate the growth of its application to help solve important biological problems in protein chemical biology.

References

1 S. D. Maleknia, M. R. Chance and K. M. Downard, *Proc. 47th ASMS Conf. Mass Spectrometry and Allied Topics*, Dallas, Texas, 1999, p. 1365.
2 D. J. Galas, *Trends Biochem. Sci.*, 2001, **26**, 690–693.
3 K. M. Downard, *Proteomics*, 2006, **6**, 5374–5384.
4 *Mass Spectrometry of Protein Interactions*, ed. K. M. Downard, Wiley-Interscience, New York, U.S.A., 2007.
5 L. Konermann, X. Tong and Y. Pan, *J. Mass Spectrom.*, 2008, **43**, 1021–1036.
6 F. Zappacosta, A. Pessi, E. Bianchi, S. Venturini, M. Sollazzo, A. Tramontano, G. Marino and P. Pucci, *Protein Sci.*, 1996, **5**, 802–813.
7 M. Monti and P. Pucci, in *Mass Spectrometry of Protein Interactions*, ed. K. M. Downard, Wiley-Interscience, New York, U.S.A., 2007.
8 Z. Zhang and D. L. Smith, *Protein Sci.*, 1993, **2**, 522–531.
9 L. Konermann, J. Pan and Y. H. Liu, *Chem. Soc. Rev.*, 2011, **40**, 1224–1234.
10 J. W. Back, L. de Jong, A. O. Muijsers and C. G. Koster, *J. Mol. Biol.*, 2003, **331**, 303–313.
11 A. Sinz, *Mass Spectrom. Rev.*, 2006, **25**, 663–682.
12 S. D. Maleknia, M. R. Brenowitz and M. F. Chance, *Anal. Chem.*, 1999, **71**, 3965–3973.
13 S. D. Maleknia, M. R. Chance and K. M. Downard, *Rapid Commun. Mass Spectrom.*, 1999, **13**, 2352–2358.
14 N. Baichoo and T. Heyduk, *Biochemistry*, 1997, **36**, 10830–10836.
15 S. D. Maleknia, C. Y. Ralston, M. D. Brenowitz, K. M. Downard and M. R. Chance, *Anal. Biochem.*, 2001, **289**, 103–115.
16 S. D. Maleknia and K. M. Downard, *Mass Spectrom. Rev.*, 2001, **20**, 388–401.
17 H. J. H. Fenton, *J. Chem. Soc.*, 1894, **65**, 899–910.
18 S. Goldstein, D. Meyerstein and G. Czapski, *Free Radical Biol. Med.*, 1993, **4**, 435–445.
19 K. Takamoto and M. R. Chance, *Annu. Rev. Biophys. Biomol. Struct.*, 2006, **35**, 251–276.
20 B. Stokes and L. Konermann, *Anal. Chem.*, 2009, **81**, 20–27.
21 S. D. Maleknia, J. W. H. Wong and K. M. Downard, *Photochem. Photobiol. Sci.*, 2004, **3**, 741–748.
22 K. M. Downard, S. D. Maleknia and S. Akashi, *Rapid Commun. Mass Spectrom.*, 2012, **26**, 226–230.
23 S. D. Maleknia and K. M. Downard, *Rapid Commun. Mass Spectrom.*, 2012, **26**, 2311–2318.
24 J. S. Sharp, J. M. Becker and R. L. Hettich, *Anal. Biochem.*, 2003, **313**, 216–225.

25 S. D. Maleknia and K. M. Downard, in *Mass Spectrometry of Protein Interactions*, ed. K. M. Downard, Wiley Interscience, New York, 2007, ch. 6.
26 T. T. Aye, T. Y. Low and S. K. Sze, *Anal. Chem.*, 2005, **77**, 5814–5822.
27 B. B. Stocks and L. Konermann, *Anal. Chem.*, 2009, **81**, 20–27.
28 H. Zhang, B. C. Gau, L. M. Jones, I. Vidavsky and M. L. Gross, *Anal. Chem.*, 2011, **83**, 311–331.
29 S. D. Maleknia and K. Fisher, *Proc. 18th Int. Mass Spectrom. Conf.*, Bremen, Germany, 2009.
30 S. D. Maleknia and R. S. Johnson, in *Amino Acids, Peptides and Proteins in Organic chemistry*, ed. A. Hughes, Wiley Interscience, New York, U.S.A., 2011, vol. 5.
31 G. Xu and M. R. Chance, *Anal. Chem.*, 2005, **77**, 4549–4555.
32 S. D. Maleknia and K. M. Downard, *Eur. J. Biochem.*, 2001, **268**, 5578–5588.
33 L. Willard, A. Ranjan, H. Zhang, H. Monzavi, R. F. Boyko, B. D. Sykes and D. S. Wishart, *Nucleic Acids Res.*, 2003, **31**, 3316–3319.
34 J. W. Ha, A. B. Schwahn and K. M. Downard, *Rapid Commun. Mass Spectrom.*, 2010, **24**, 2900–2908.
35 A. B. Kanu, P. Dwivedi, M. Tam, L. Matz and H. H. Hill, *J. Mass Spectrom.*, 2008, **43**, 1–22.
36 E. Mack, *J. Am. Chem. Soc.*, 1925, **47**, 2468–2482.
37 S. D. Maleknia and K. M. Downard, *Eur. J. Biochem.*, 2001, **268**, 5578–5588.
38 Z. Chi and S. A. Asher, *Biochemistry*, 1998, **37**, 2865–2872.
39 B. B. Stocks and L. Konermann, *Anal. Chem.*, 2009, **81**, 20–27.
40 J. W. H. Wong, S. D. Maleknia and K. M. Downard, *Anal. Chem.*, 2003, **75**, 1557–1563.
41 S. J. Gerega and K. M. Downard, *Bioinformatics*, 2006, **22**, 1702–1709.
42 J. W. H. Wong, S. D. Maleknia and K. M. Downard, *J. Am. Soc. Mass Spectrom.*, 2005, **16**, 225–233.
43 S. C. Goldsmith, S. D. Maleknia, S. C. Almo and M. R. Chance, *Biophys. J.*, 2000, **78**, 213.
44 J. G. Kiselar, P. A. Janmey, S. C. Almo and M. R. Chance, *Proc. Natl. Acad. Sci. U. S. A.*, 2003, **100**, 3942–3947.
45 K. M. Downard, Y. Kokabu, M. Ikeguchi and S. Akashi, *FEBS J.*, 2011, **278**, 4044–4054.
46 H. Diemer, C. Atmanene, S. Sanglier, B. Morrissey, A. Van Dorsselaer and K. M. Downard, *J. Mass Spectrom.*, 2009, **44**, 803–812.
47 E. R. Stadtman, *Free Radical Res.*, 2006, **40**, 1250–1258.
48 W.-K. Shum, S. D. Maleknia and K. M. Downard, *Anal. Biochem.*, 2005, **344**, 247–256.
49 S. Issa and K. M. Downard, *J. Mass Spectrom.*, 2006, **41**, 1298–1303.
50 S. D. Maleknia, N. Reixach and J. N. Buxbaum, *FEBS J.*, 2006, **273**, 5400–5406.

